lar excited states which heretofore would have escaped detection. This in turn allows us to make a comparison between the value of the excited-state coupling parameter determined by experiment and the value predicted by quantum chemistry calculations. Presently, our knowledge of the structure of short-lived excited states of molecules is exceedingly primitive compared to that of ground states. The methods of level-crossing and optical double-resonance experiments permit us to study excited states with a precision approaching that of microwave, esr, and molecular-beam resonance studies of ground and metastable states. As with almost all molecular spectroscopy, the contribution of these interference methods to our chemical understanding seldom comes from one measurement, but rather is a cumulative process depending upon our ability to interpret the trends that emerge in terms of "chemical shifts," used in the broadest sense of the meaning. The application of interference techniques to probe the charge distributions of molecular excited states is a fairly recent development. Already, as shown in Table I, excitation by atomic line coincidences, molecular resonance lamps, white light sources, selected laser lines, and even electron impact has proven successful in stimulating interference effects in molecular emissions. As additional means are found to extend these techniques to transient molecular species, the field may be expected to grow rapidly.

Support by the National Science Foundation is gratefully acknowledged.

Some Aspects of Small-Angle X-Ray Scattering

GEORGE W. BRADY

Bell Laboratories, Murray Hill, New Jersey 07974

Received January 11, 1971

In this Account we will discuss the techniques of small-angle X-ray scattering as applied to structural problems of the liquid state. There are, of course, other areas in which the method is of great use,[1-3] but we will limit ourselves to the studies of inhomogeneities in liquids and of scattering phenomena which occur at or near critical points and phase transitions.

As its name implies, small-angle scattering designates that part of the intensity pattern which is observed in the vicinity of the main beam. Its angular limits will be defined later. It was first noticed or reported in the 1930's, notably by Bernal[4] and coworkers in their work on tobacco mosaic virus, and by Krishnamurti and Warren,[5] who studied carbon black. The first detailed investigation of the phenomenon was made by Guinier,[6-8] who was interested in studying that part of the X-ray intensity pattern which lies between the Bragg peaks.

To do this, great care had to be taken to remove all extraneous scattering from the weak intensity patterns, and it was an experimental triumph when Guinier's painstaking efforts brought this about. One of the main sources of this unwanted scattering was the presence of the continuous spectrum in the target beam. To isolate the characteristic Kα line and still obtain sufficient intensity, a curved crystal monochromator had to be used. This had the added result of focusing the incident beam to a small angle, thus allowing the isolation of a scattered spectrum which was centered around zero. Elimination of air and slit scattering further reduced the background.

After the carbon black measurements of Warren were confirmed, a search for the origin of the scattering was begun. A study of silica in the vitreous state (no small-angle scattering) and in a gel (small-angle scattering) indicated immediately that the scattering arose from inhomogeneities of a mean size much greater than that of interatomic spacings (which give rise to the usual Bragg peaks). In fact, they were of the order of the grain size of the silica gel.

This result demonstrated for the first time that X-rays could be used for determination of the morphology of relatively large aggregates or molecules, of the order of tens to thousands of ångströms.

Guinier[8] soon developed a theory for the phenomenon which gave a simple relation between the intensity and the radius of gyration $\bar{R}$. $\bar{R}$ is the average distance of the electron density distribution from the center of charge. Thus for a large molecule or particle

$$\bar{R}^2 = \frac{\int \rho(r) r^2 \mathrm{d}v}{\int \rho(r) \mathrm{d}v} \tag{1}$$

where $\rho(r)$ is the electron density at a distance r and v is the volume of the particle. The relation is

$$I \sim e^{-s^2\bar{R}^2/3} \tag{2}$$

where $s = 4\pi/\lambda \sin\theta$; λ is the wavelength, and θ is one-half the scattering angle.

(1) The literature on small angle scattering has grown large, but strangely enough the only textbook in the field, "Small Angle Scattering of X-Rays," by Guinier, *et al.*, J. Wiley and Sons, New York, 1955, is out of print. The best survey of the field up to 1965 is given in ref 2. An up-to-date bibliography is given in ref 3.

(2) H. Brumberger, Ed., "Small Angle X-Ray Scattering," Gordon and Breach, New York, London, and Paris, 1967.

(3) A. J. Renouprez, *Int. Union Crystallogr., Comm. Crystallogr. App., Bibliogr.*, **No. 4** (1970).

(4) J. D. Bernal and I. Fankuchen, *J. Gen. Physiol.*, **25**, 111 (1941).

(5) P. Krishnamurti, *Indian J. Phys.*, **5**, 473 (1930); B. E. Warren, *J. Chem. Phys.*, **2**, 551 (1934).

(6) A. Guinier, *C. R. Acad. Sci.*, **206**, 1641 (1938).

(7) A. Guinier, *Ann. Phys. (Paris)*, **12**, 161 (1939).

(8) A. Guinier, *Phys. Today*, **22**, 25 (1969); see also ref 1-3.

While this relation is only true for a random arrangement of discrete entities, with no interference (such as a dilute solution of macromolecules or a colloidal suspension), it is worthwhile discussing it briefly before going on to the more general theory of Debye.[9] Equation 2 shows that the intensity will have a maximum in the forward direction, decreasing rapidly on either side of zero angle. As a rough estimate[10] the scattering will be negligible at a scattering angle 2θ greater than $\lambda/\bar{R}$. Thus for $\lambda = 1.5$ Å and $\bar{R} = 100$ Å the scattering will be contained within an angle of 0.015 radian, or 1°. With present techniques, measurements can be made into angles as small as ~15 sec of arc, corresponding to $\bar{R}$ values of 15–20,000 Å.

As eq 1 shows, the density distribution does not have to be uniform over $\bar{R}$ and thus the atomic arrangement does not influence the intensity pattern. In fact, small-angle scattering has nothing to do with structure in the crystallographic sense. It is an application of the principles of optical interference and diffraction and is valid for any wavelength. The particles must be quite uniform in size and shape, otherwise eq 2 is invalid. In the case of uniform particles, once $\bar{R}$ is evaluated, the shape[10] and specific surface can be determined from the tails of the scattering curve.

The theory was put on a more rigid basis by Debye[9] and Porod.[11] Their approach was essentially the same in that they used a correlation function to express the extent of fluctuations in electron density. The physical meaning of the correlation function is straightforward and is in fact the extension or analog of the Patterson function of crystallography. Take any two volume elements at distances r_m and r_n from any arbitrary point in the system. Suppose that there exist at these points electron density fluctuations $\delta\rho_m$ and $\delta\rho_n$ superimposed on the average density ρ. Their product, averaged over time, is $\langle(\delta\rho_m/\rho)/(\delta\rho_n/\rho)\rangle$. For $r_n - r_m = 0$, $\delta\rho = \delta\rho_m = \delta\rho_n$ and the product is $\langle(\delta\rho/\rho)^2\rangle$. By introducing a function, $G(r)$, the fluctuations at $r = 0$, r_m, and r_n are correlated. Thus

$$\left\langle \left(\frac{\delta\rho_m}{\rho}\right)\left(\frac{\delta\rho_n}{\rho}\right)\right\rangle = G(r)\left\langle \left(\frac{\delta\rho}{\rho}\right)^2\right\rangle \qquad (3)$$

We note that $G(r)$ in eq 3 does the following. (1) It becomes unity for $r = 0$, since the fluctuation correlates with itself. It tends to zero for large values of r. (2) For all values of $r_n - r_m$, the vector $r_n - r_m$, with fixed length, successively takes up all positions in the sample. The correlation function thus compares the fluctuation product of this distance with the square of the average fluctuation at any single point. (3) $G(r)$ can assume negative values when the time-average values of the fluctuations at two points are of opposite sign. (4) In the case of a solid (isotropic) the fluctuations are considered to be frozen in. The correlation function becomes a space average.

The correlation function contains all the information derivable from the experiments and is essentially the Fourier transform of the intensity. For example, consider the case of an isolated sphere. The problem in this case reduces to calculating the probability that a point in the sample at a distance r from a point in the sphere is itself in the sphere. The integral of the correlation function then reduces to the Rayleigh scattering function for a sphere.

The correlation length, the distance over which the fluctuations are correlated, replaces the radius of gyration concept and is found to be the average length of all lines passing through the particle and terminating on its boundary.

The complexity of the liquid state tends to make the interpretation of the scattering results less straightforward, and some care must be taken in setting up experiments to isolate the phenomenon one wishes to measure. This makes the field more interesting since the technique is so inherently powerful.

Theory

The equations for small-angle scattering[10] can be derived from the Debye expression[12] which shows that the intensity in electron units scattered at an angle 2θ by an assembly of atoms is given by eq 4. Here f_m and f_n

$$I(s) = \sum_m \sum_n f_m f_n \frac{\sin sr_{mn}}{sr_{mn}} \qquad (4)$$

are the scattering factors of atoms m and n, and r_{mn} is the distance between them. The factors f_m and f_n are the scattering of these atoms relative to that of a single electron, and $s = (4\pi/\lambda)\sin\theta$, where λ is the wavelength. When applied to the small-angle region, f_m and f_n are replaced by $\rho_m dv_m$ and $\rho_n dv_n$, where ρ_m and ρ_n are the average electron densities in the volume elements dv_m and dv_n. We can then write eq 5, where V is

$$I(s) = \int\int \rho_m\rho_n \frac{\sin sr_{mn} dV_m dV_n}{sr_{mn}} \qquad (5)$$

the sample volume. The only step left is to introduce the correlation function. This is done directly by writing $\rho_m = \rho + (\delta\rho_m/\rho)$ and $\rho_n = \rho + (\delta\rho_n/\rho)$ with the restriction that $\int\delta\rho_m dv_m = 0$. Substituting in eq 5

$$I = I_e \times \int_V \int_V \left[\rho + \left(\frac{\delta\rho_m}{\rho}\right)\right]\left[\rho + \left(\frac{\delta\rho_n}{\rho}\right)\right] \frac{\sin sr_{mn}}{sr_{mn}} dv_m dv_n \qquad (6)$$

When multiplied out three terms result, the first two of which are seen to be negligible in the observable small-angle regions.[1] It follows that

$$I = I_e \int_V \int_V \left(\frac{\delta\rho_m}{\rho}\right)\left(\frac{\delta\rho_n}{\rho}\right) \frac{\sin sr_{mn}}{sr_{mn}} dv_m dv_n \qquad (7)$$

This expression can be simplified further and its meaning made clearer by examining the integral with respect to r_m. Remembering that $r_n = r_m + r_{nm}$ and that we have

(9) P. Debye and A. M. Bueche, *J. Appl. Phys.*, **20**, 518 (1949).
(10) W. W. Beeman, P. Kaesberg, J. W. Anderegg, and M. B. Webb, *Handb. Phys.*, **32**, 321 (1957).
(11) G. Porod, *Kolloid-Z.*, **124**, 83 (1951); **125**, 109 (1952).
(12) P. Debye, *Ann. Phys. (Leipzig)*, **46**, 809 (1915).

assumed spherical symmetry, the integral is $\int_V (\delta\rho_m/\rho)\cdot(\delta\rho_{m+mn}/\rho)\mathrm{d}v_m$. It is a function of r_{mn} only. For each value of r_{nm} and the corresponding fluctuation ρ_{m+mn} we integrate the fluctuation product as $\mathrm{d}v_m$ moves over the volume V. For $r_{mn} = 0$ the value of the integral is $\langle(\delta\rho/\rho)^2\rangle V$. When $r_{mn} \neq 0$, there is no analytical solution because it is impossible to assess the simultaneous values of $\delta\rho$ at two points in the system. We therefore denote the integral by $G(r)$, with the coefficient $\langle(\delta\rho/\rho)^2\rangle V$ to generate the value at $r_{mn} = 0$. Equation 7 then becomes

$$I = I_e\left(\frac{\delta\rho}{\rho}\right)^2 V\int G(r)\,\frac{\sin sr}{sr}\,4\pi r^2\mathrm{d}r \qquad (8)$$

where for convenience we have dropped the subscripts. This is the final expression for the scattering. As pointed out in the introduction, $G(r)$ can be obtained by a Fourier transformation of this equation. For technical reasons which we will not discuss further, eq 8 is not generally used directly. It can, however, be expanded in the region of small s to give eq 9. The second term

$$\frac{I(s)}{I(s=0)} = 1 - \frac{\int r^2G(r)\mathrm{d}v}{\int G(r)\mathrm{d}v}\,\frac{s^2}{6} \qquad (9)$$

defines a length, L (eq 10), the persistence or correlation length. This important quantity can then be obtained directly from experiment. Debye[13] has shown that in certain liquids it can be related to the range of intermolecular forces.

$$L^2 = \frac{\int r^2G(r)\mathrm{d}v}{\int G(r)\mathrm{d}v} \qquad (10)$$

Methods

The experimental techniques are sophisticated, and a satisfactory discussion of them is beyond the scope of this Account. In fact, the growth of the field has to a large extent been determined by the rate of development of adequate equipment. The reader is referred to articles by Kratky[14] and Bonse and Hart[15] for a reasonably up to date survey of these aspects. In essence a measurement involves first an accurate determination of the scattering pattern. The intensity is generally quite low, of the order of 1 count/sec. Next, the data must be "desmeared." This term refers to the operation of converting the measured data as far as possible to that which would be obtained with an infinitely small slit system. Computer programs are available for this.[16,17] It is a necessary step because the small total angular range covered seriously limits the allowed angular divergence. To give some idea of the precision available with modern techniques, Figure 1 shows the scattering patterns from a dried sample of Dow polystyrene latex,[18] obtained with a modified Bonse–Hart slit system.[17] This compound as bought is an emulsion of uniform spheres. The three curves are (1) the experimentally determined curve, (2) curve 1 after the desmearing operation, and (3) the theoretical Rayleigh scattering function for spheres. As can be seen from the figure, in an angular range of 0 to 30 min of arc from the main beam 12 peaks are resolved. The diameter of the latex spheres, determined from the position of the maxima of the last 10 peaks, is 2498 ± 9 Å, or an accuracy of ~0.4%.[18]

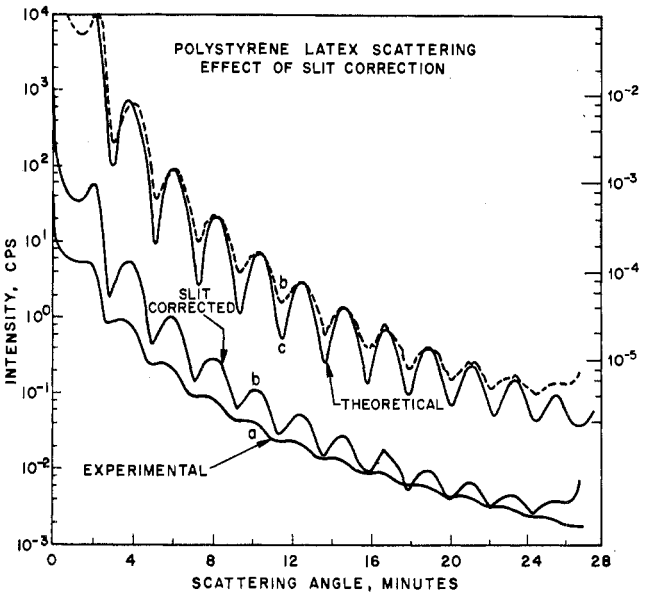

Figure 1. Scattering curve for Dow polystyrene latex (modified Bonse–Hart apparatus): curve 1, experimental curve; curve 2, slit-desmeared curve; curve 3, theoretical Rayleigh scattering function for spheres.

Results and Discussion

The perfluoroheptane–isooctane system[19] is interesting from a thermodynamic viewpoint in that regular solution theory[20] predicts a consolute temperature of −203°, whereas the measured value is 23.78°. In addition, the Zimm clustering function[21,22] (defined for a binary solution of A, B molecules as the mean number of molecules A in excess of random expectation in the vicinity of a given molecule A) is large and positive in a ~25% composition interval around the critical concentration. From a small-angle X-ray point of view this phenomenon should be amenable to investigation because of the large difference in scattering power of the two components.

Figure 2[19] shows the scattering curves for different values of the volume fraction φ_2 of C_7F_{16} at $T = 28.3°$. At $\varphi_2 = 0.12$ there is already evident a faint scattering;

(13) P. Debye, *J. Chem. Phys.*, **31**, 680 (1959).
(14) O. Kratky, "Small Angle X-Ray Scattering," H. Brumberger, Ed., Gordon and Breach, New York, N. Y., 1967, Chapter 4.
(15) U. Bonse and M. Hart, *Appl. Phys. Lett.*, **6**, 155 (1965).
(16) P. W. Schmidt and J. Hight, Jr., *Acta Crystallogr.*, **13**, 480 (1960).
(17) C. C. Gravatt and G. W. Brady, *J. Appl. Crystallogr.*, **2**, 289 (1969).
(18) U. Bonse and M. Hart, *Z. Phys.*, **189**, 151 (1966); C. C. Gravatt and G. W. Brady, in press.
(19) G. W. Brady, *J. Chem. Phys.*, **32**, 45 (1960).
(20) J. Hildebrand, R. Fisher, and M. Benesi, *J. Amer. Chem. Soc.*, **72**, 4348 (1950); J. Hildebrand and R. L. Scott, "Solubility of Non-Electrolytes," Reinhold, New York, N. Y., 1950.
(21) B. H. Zimm and J. L. Lundberg, *J. Phys. Chem.*, **60**, 425 (1956).
(22) C. R. Mueller and J. E. Lewis, *J. Chem. Phys.*, **26**, 286 (1957); criticized by A. G. Williamson, R. L. Scott, and R. D. Dunlap, *ibid.*, **30**, 325 (1959).

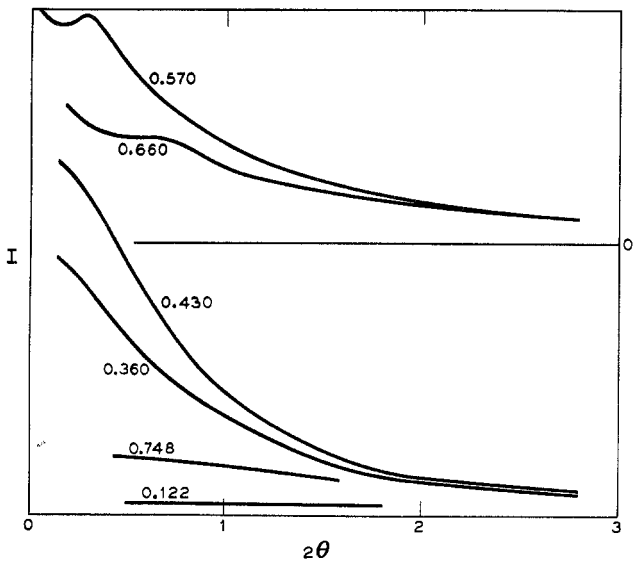

Figure 2. Scattering from the C_7F_{16}–i-C_8H_{18} system for various values of φ_2, the volume fraction of C_7F_{16}. The abscissa is in degrees of arc.

it increases markedly as the volume fraction increases. Of the curves measured, that for $\varphi_2 = 0.43$ shows the maximum intensity and slope. Beyond this, at the intermediate concentrations, interference peaks appear. Finally the curve becomes smooth again at 0.75 with a decrease in slope and intensity.

We can interpret the behavior of these curves as being due to one or both components tending to surround themselves with their own kind. [It is the absolute value of $(\rho - \rho_0)$ which gives rise to the scattering.] Qualitatively it would seem that starting at a low concentration C_7F_{16} molecules segregate into "clusters" which increase in size and number with concentration. At the middle concentrations the distribution of clusters can no longer be considered as random, and the peaks result from this. The decrease in slope at the highest concentration could be explained on the basis of a phase reversal having taken place such that clusters of hydrocarbon in a continuous fluorocarbon phase are being observed.

Values of L, calculated from the scattering curves, are listed in Table I, along with values of $T - T_c$, the temperature above the consolute curve. We note that the temperature interval over which the phenomenon is observed is considerable, indicating that the transition, or critical region, between the one- and two-phase region is quite large. This can be seen in more detail in Figure 3,[23] where the correlation lengths as a function of temperature are shown for the 30 and 40% solutions. It is evident that the correlations extend to fairly large distances, of the order of 40 Å, at temperatures at least as high as 16° above the transition temperature. Also interesting is the way L increases as the temperature is lowered. It rises to an apparent maximum at a point about 1° above the consolute curve, then flattens out until the separation temperature, which occurs at the lower end of this region, is reached. After separation

(23) G. W. Brady and H. L. Frisch, *J. Chem. Phys.*, **37**, 1514 (1962).

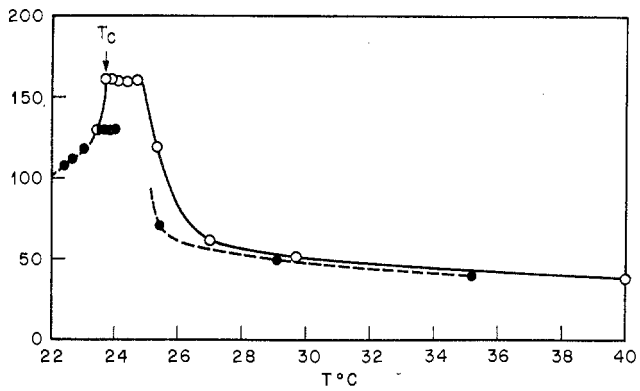

Figure 3. Persistence lengths L plotted as a function of temperature. T_c is the temperature at which two phases appear. Solid line, 40% C_7F_{16}; dashed line, 30% C_7F_{16}.

Table I
Values of L and $T - T_c$ for the Different Values of φ_2

φ_2, deg	$T - T_c$, °C	L, Å
0.12	19	10.2
0.36	5	40.6
0.43	4	40.6
0.57	5	
0.66	7	
0.75	13	17.3

both curves superimpose, the ordinate of the curve for the higher concentration dropping rapidly after 23.75° until the separation temperature, 23.44°, of the lower concentration is reached. This is consistent with the phase diagram,[19] which indicates that after phase separation the composition depends uniquely on temperature.

At the critical concentration, 41.5% C_7F_{16}, the first derivative of the activity isotherm is zero, analogous to a one-component system where the compressibility becomes infinite, and thus the correlations become very long range.[24,25] The X-ray scattering is of course directly related to the correlation function, whose behavior under critical conditions is the quality deduced from the various models. Debye,[13] in a reformulation of the Ornstein–Zernike[26] theory, concluded that a correlation function of the form

$$G(r) \sim \frac{e^{-\beta r}}{r} \tag{11}$$

with $\beta(T)$ vanishing at T_c was in agreement with experiment. Later developments,[27,28] using lattice gas[29] and cluster algebra[30,31] techniques, indicate that this result is not quite correct, and that $G(r)$ should be written as

(24) G. W. Brady, D. McIntyre, M. E. Myers, Jr., and A. M. Wims, *ibid.*, **44**, 2197 (1966).
(25) G. W. Brady, D. McIntyre, M. E. Myers, Jr., and A. M. Wims, "Small Angle X-Ray Scattering," Gordon and Breach, New York, N. Y., 1967, Chapter 22.
(26) L. S. Ornstein and F. Zernike, *Proc. Acad. Sci. (Amsterdam)*, **17**, 793 (1914).
(27) H. Brumberger, *Nat. Bur. Stand. (U.S.), Spec. Publ.*, **No. 273**, (1966).
(28) A. Munster in "Fluctuation Phenomena in Solids," R. Burgess, Ed., Academic Press, New York, N. Y., 1965. See also ref 27.
(29) M. Fisher, *J. Math. Phys. (New York)*, **5**, 944 (1964).
(30) J. M. J. Van Leeuven, J. Groeneveld, and J. DeBoer, *Physica*, **25**, 792 (1959).
(31) M. S. Green, *J. Chem. Phys.*, **33**, 1403 (1949).

$$G(r) \sim \frac{1}{r^{1+\epsilon}} \qquad (12)$$

where $1 \geq \epsilon > 0$. A $G(r)$ of the form of eq 12 leads to an expression[29] (eq 13) for the critical scattering. Thus

$$I(s) \sim \frac{1}{[B^2(T) + S^2]^{1-(\epsilon/2)}} \qquad (13)$$

a plot of $I^{-1/1-(\epsilon/2)}$ against s^2 will give a straight line if a proper choice of the exponent ϵ is made, and thus gives a means for determining its value.

The $I^{-1/1-(\epsilon/2)}$ plots are shown in Figure 4.[25] Starting from a value of zero for curve d, ϵ increases to 0.04 for curve c and reaches a constant value of 0.10 for the two lowest temperatures, whose plots are virtually indistinguishable. Experimentally then, the lattice gas appears to be a satisfactory approach for interpreting the results. Thus, as predicted by Fisher[29] and Frisch and Brady,[32] eq 13 formulation is valid, not close to T_c, the region to which it was supposed to apply,[26] but at temperatures in the critical region removed from it. Also, Fisher's[33] calculations of a cubic lattice gas lead to a value of $\epsilon = 0.08$, very close to 0.1, our measured value. Finally, the fact that a system of fairly complicated molecules such as this one can be described by a simple lattice model points up the insensitivity of $G(r)$ to the details of the local potential.

We discuss next the results of a similar set of experiments on *p*-azoxyanisole, a typical one-component liquid crystal system.[34,35] This compound forms a liquid crystal phase on melting which persists until a transition temperature, T_c (138.53°), is reached, at which point the turbid phase changes discontinuously into a normal clear liquid. The transition has a latent heat of 178 cal/mole and is presumably first order. Our aim was to study premonitory phenomena as the transition was approached from the isotropic liquid side.

Figure 5 shows the scattering curves. Even at $T \sim 152°$ ($T_c + 16°$) there is development of excess scattering, giving evidence for long-range molecular ordering. As T approaches T_c the excess scattering increases in intensity, and moves to smaller angles, indicating that $G(r)$ is becoming longer ranged. The curves at 141.50°, 137.70°, and 135.83° show this clearly. Below 135.83° the scattering patterns superimpose throughout the nematic region; the transition is thus complete at this temperature. Values of the correlation length, determined from Guinier plots, are listed in Table II along with an estimate of the number of molecules in the correlated regions. The table shows that L increases rapidly from an initial value of 300 Å up to ~1850 Å at the transition, in a temperature interval of ~16°, an effect similar to that observed for the critical phenomenon.

The physical picture of the behavior of $G(r)$, or L, is not as clear here as in the two-component case. The formation of regions of nematic material would certainly produce a density difference (although the bulk density and volume changes are small). The lack of interference peaks in the smooth Guinier plots for L would indicate that widely separated uniform regions of different scattering power could be present. This was not an unambiguous interpretation, however. A series of experiments with different windows eliminated surface ef-

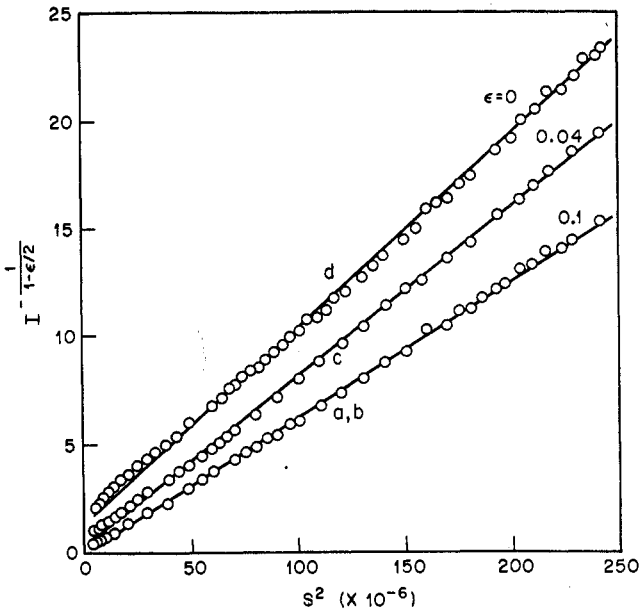

Figure 4. OZ plots of the critical scattering from C_7F_{16}–*i*-C_8H_{18}. The values of $\Delta T = T - T_c$ are: curve a, 0.007°; curve b, 0.20°; curve c, 0.125°; curve d, 0.306°.

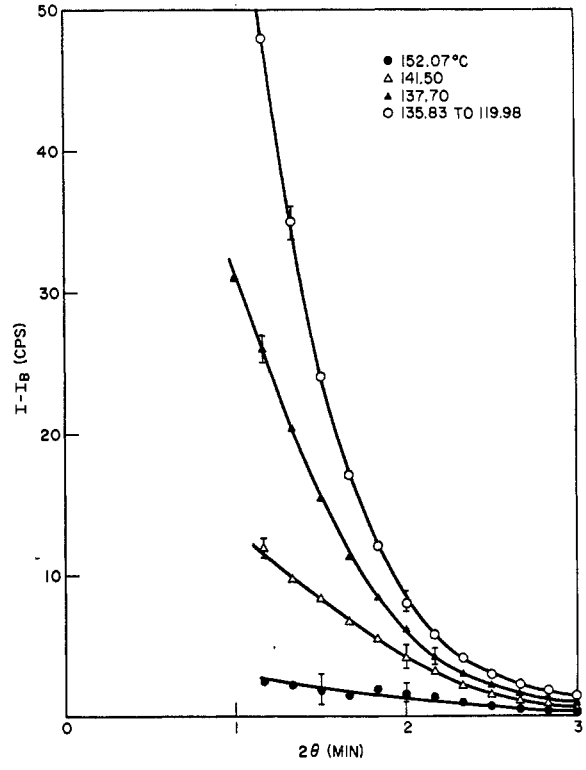

Figure 5. Excess scattering from *p*-azoxyanisole for temperatures above and within the nematic region.

(32) H. L. Frisch and G. W. Brady, *J. Chem. Phys.*, **37**, 1514 (1962).
(33) M. E. Fisher and R. J. Burford, *Phys. Rev.*, **155**, 583 (1967).
(34) C. C. Gravatt and G. W. Brady, *Mol. Cryst. Liquid Cryst.*, **7**, 355 (1969).
(35) C. C. Gravatt and G. W. Brady, "Liquid Crystals and Ordered Fluids," Plenum Press, New York, N. Y., 1970, p 458.

Table II
Correlation Lengths Determined from the Data of Figure 6

T, °C	L, Å	N_s
152.07	300^{+400}_{-300}	$<10^3$
141.50	1000^{+150}_{-300}	8×10^4
137.70	1500 ± 150	2×10^5
135.83–129.93	1850 ± 75	10^6
122.10	1900 ± 150	
119.98	1900^{+300}_{-200}	

fects as a factor. Impurity effects were then investigated. This was done by replacing the British Supply House 99% pure *p*-azoxyanisole used in the experiments by zone-refined 99.99% James Hinton Co. material and making an extensive set of measurements similar to those described above. Repeat runs on the 99% material were also done.

The differences between the two series of sample runs were unmistakable. The pure Hinton (99.99%) material showed no change at all in the scattering patterns over the temperature range from 160 to 120°, and in particular no change near T_c, although the phase transition could be observed optically, and no supercooling was noted. Thus no excess scattering over background (the 160° curve) was present, indicating that correlation effects were undetectable. The repeat runs on the 99% material reproduced the results of Figure 6. Perhaps as interesting, after a number of measurements on the 99.99% material, excess scattering would develop and it would then take a period of 24 hr before the intensity patterns stabilized. After this time the sample gave results similar to those shown in Figure 5. A further series of experiments on cholesteryl bromide, both pure and slightly decomposed, showed no scattering, with the conclusion that the impurity effect manifested itself in the nematic material only.

It seems plausible then that perhaps the origin of the scattering lies in the existence of disclination lines or domain boundaries which nematic liquid crystal phases possess and the cholesteric phases do not. Our current thinking is that the nematic threads act as segregation sites for the impurities, producing either an excess or a deficiency of electron density, and that the observed correlation lengths are a measure of this. Such an interpretation would explain why such small amounts of impurity produce such marked effects because the threads take up a part of the total volume of the same order of magnitude as that of the impurities. We definitely do not mean to imply that the impurities cause the thread formation.

Finally, a plot of I^{-1} against s^2 in the manner of Figure 4 showed an upward concavity at small s^2. This would imply a negative ϵ, which is physically impossible, and thus all transition orders but the first are ruled out.

As in standard diffraction, substitution techniques have been found to be of great use in small-angle studies.[36-39] We content ourselves with presenting results of some experiments we have done on long-chain alkane molecules in solution.[40,41] High atomic number atoms are substituted at positions in the molecule to enhance the scattering from some structural feature. This scattering is then compared with that of a solution of the same atomic composition in which that structural feature is absent. For example, to determine the end-to-end distance of a long-chain polymeric molecule containing $n + m$ carbon atoms we measure the pattern of a (α, ω) diiodide solution ($C_{n+m}I_2$ + solvent) and compare it with that of a 1-iodo solution ($C_nI + C_mI$ + solvent) of equivalent composition. Subtracting the latter from the former should leave only the contribution of the I atoms at the end of the C_{m+n} chain. This reduces the Debye[12] equation to

$$I_D = f^2 I \sum a_m \frac{\sin sr_m}{sr_m}$$

where r_m is the distance between the terminal I atoms. The summation over a_m and r_m, with $\Sigma a_m = 1$, takes into account a spread in distances around a most probable one, which is normally the state of affairs in liquids.

The studies were made on[40] a series of alkanes varying in chain length from C_8 to C_{22}, with decalin, $C_{10}H_{18}$,

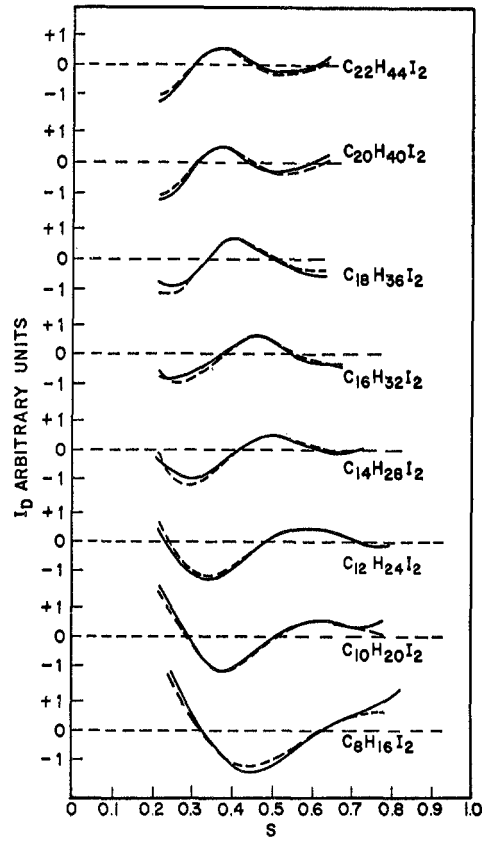

Figure 6. Intensity difference patterns for alkane solutions. Full curves, experimental; dashed curves, calculated.

(36) O. Kratky and W. Worthman, *Monatsh. Chem.*, **76**, 263 (1947).
(37) O. Kratky, G. Porod, and A. Sekora, *ibid.*, **78**, 295 (1948).
(38) G. W. Brady, R. Salovey, and J. M. Reddy, *Biopolymers*, **3**, 573 (1965).
(39) G. W. Brady and R. Salovey, *ibid.*, **5**, 331 (1967).
(40) G. W. Brady, C. Cohen-Addad, and E. F. X. Lyden, *J. Chem. Phys.*, **51**, 4320 (1969).
(41) G. W. Brady, C. Cohen-Addad, and E. F. X. Lyden, *ibid.*, **51**, 4309 (1969).

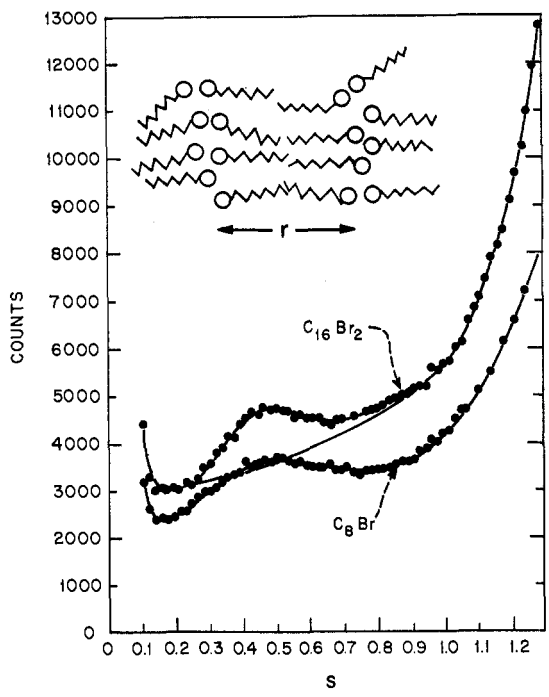

Figure 7. Intensity pattern of a dibromide, $C_{16}H_{32}Br_2$, and a monobromide, $C_8H_{17}Br$, of half the corresponding alkane chain length showing the existence of peaks in the intensity patterns at roughly the same angle. A crude model of the alignment is included. The circles are halogen atoms.

as solvent. A proper analysis of the data required a knowledge of the contributions to the intensity of the distribution functions of solvent and solute molecules with respect to themselves and each other. This could be obtained experimentally; in Figure 6, I_D, the function which measures the end-to-end I–I interaction, isolated from all the others, is shown. The full lines are the measured values and the dashed lines the calculated distribution. It is found that the width of the latter is ± 2 Å and that the $\langle r_m \rangle$ values are in good agreement with those deduced by Flory from a rotational isomeric treatment. Full details are to be found in the original papers.[40,41]

A surprising result of the investigation[40] was the large amount of order present in the monoiodide solutions. This is illustrated in Figure 7, which shows a trace of the region of the intensity pattern of 1-bromooctane, where the corresponding 1,16-dibromohexadecane shows a peak. Clearly indicated is some type of quasi-liquid crystal behavior in which the long-chain molecules line up in such a way that the halogen atoms make maximum contact with each other, as do the chains themselves. We have established[42] the following. (1) The strong ordering tendency of the long-chain molecules persists when solvent is added. It becomes noticeably evident in the intensity pattern at concentrations of ~6 mole %. (2) In solutions of molecules of one chain length, C_mX, where X is a halogen, the peak occurs in the distance range corresponding to a length $\sim C_{2m}$. (3) In solutions of molecules of $C_mX + C_nX$, the distance range corresponds to C_{2m}, where m is the length of the longest chain. When the length C_m approaches the length C_n, the peak corresponds to a length C_{m+n}. Thus, a solution of C_2X and $C_{20}X$ alkanes gives a peak at $\sim C_{40}$. On the other hand, a $C_{10} + C_{12}$ solution exhibits a peak at C_{22} (10 + 12). (4) The peaks for the monosubstituted species are quite broad, while the α,ω-disubstituted compounds produce a relatively sharp peak characteristic of a well-defined distance.

In summary, by discussing sets of measurements on three different phenomena we have tried to present a brief representative survey of our work on small-angle scattering methods as applied to the liquid state.

(42) G. W. Brady, manuscript in preparation.

Chemical Effects of Nuclear Transformations in Mössbauer Spectroscopy

GUNTHER K. WERTHEIM

Bell Laboratories, Murray Hill, New Jersey 07974

Received December 7, 1970

Since its discovery[1] in 1958 the Mössbauer effect[2,3] has become an increasingly valuable spectroscopic technique.[4] It offers not only information comparable to that obtained from nuclear magnetic or nuclear quadrupole resonance but also unique ways of determining valence and studying covalency and lattice vibrations.

The effect is based on the resonant nuclear scattering of γ rays by atoms in solids. Only γ rays which have been emitted without recoil and therefore have the full energy of the nuclear transition can be resonantly scattered. The existence of such "recoil-free" γ rays can be understood in terms of the Debye–Waller factor, familiar from X-ray crystallography. They occur whenever the free atom recoil energy is smaller than the Debye energy, $k\theta_D$. Isotopes exist in which the majority of γ rays are emitted without recoil, making the Mössbauer effect a major one.

(1) R. L. Mössbauer, *Z. Physik*, **151**, 124 (1958); *Naturwissenschaften*, **45**, 538 (1938).
(2) H. Frauenfelder, "The Mössbauer Effect," W. A. Benjamin, New York, N. Y., 1962.
(3) G. K. Wertheim, "Mössbauer Effect, Principles and Applications," Academic Press, New York, N. Y., 1964.
(4) R. H. Herber, *Annu. Rev. Phys. Chem.*, **17**, 261 (1966). See also "Chemical Applications of Mössbauer Spectroscopy," V. I. Goldanskii and R. H. Herber, Ed., Academic Press, New York, N. Y., 1968.